

Supplementary Materials

Supplementary Figure Legends

Figure S1. Clusters of major immune cell populations in the YA and AA groups derived from scRNA-seq data.

- A. t-SNE projections of PBMCs derived from scRNA-seq data in cohort-1.
- B. t-SNE plots segregated into YA and AA groups.
- C. t-SNE projection of canonical markers, including *CD3E*, *CD4*, *CD8A*, *STMN1*, *NCAM1*, *NKG7*, *CD19*, *MS4A1*, *CD14*, *FCGR3A*, *HLA-DRA*, *CD1c*, *MZB1*, *CLEC4C*, *HBB*, *PF4*.

Figure S2. Clusters of major immune cell populations in the YA and AA groups derived from mass cytometry data.

- A. t-SNE projections of PBMCs derived from mass cytometry data in cohort-1.
- B. t-SNE plots segregated by YA and AA groups.
- C. t-SNE projection of canonical markers, including *CD3*, *CD4*, *CD8A*, *CD11C*, *CD56*, *CD57*, *CD19*, *CD20*, *CD14*, *CD16*, *HLA-DRA*, *CD123*.
- D. Heatmap showing mean population expression levels of all markers.

Figure S3. Re-clustering of cell subsets derived from scRNA-seq data in cohort-1.

- A. t-SNE projections of CD3⁺ T cell subsets.
- B. t-SNE projections of CD4⁺ T cell subsets.
- C. t-SNE projections of CD8⁺ T cell subsets.
- D. t-SNE projections of NK cell subsets.
- E. t-SNE projections of B cell subsets.
- F. t-SNE projections of monocyte subsets.
- G. t-SNE projections of DC subsets.
- H. t-SNE projection of canonical markers in T cell subsets.
- I. t-SNE projection of canonical markers in CD4⁺ T cell subsets.
- J. t-SNE projection of canonical markers in CD8⁺ T cell subsets.
- K. t-SNE projection of canonical markers in NK cell subsets.
- L. t-SNE projection of canonical markers in B cell subsets.
- M. t-SNE projection of canonical markers in monocyte subsets.
- N. t-SNE projection of canonical markers in DC subsets.

Figure S4. Re-clusters of cell subsets derived from mass cytometry data in cohort-1.

- A. t-SNE projections of T cell subsets.
- B. t-SNE projections of NK cell subsets.
- C. t-SNE projections of B cell subsets.
- D. t-SNE projections of monocyte subsets.
- E. t-SNE projections of DC subsets.
- F. t-SNE projection of canonical markers in T cell subsets.
- G. t-SNE projection of canonical markers in NK cell subsets.
- H. t-SNE projection of canonical markers in B cell subsets.
- I. t-SNE projection of canonical markers in monocyte subsets.
- J. t-SNE projection of canonical markers in DC subsets.
- K. Heatmap showing mean population expression levels of all markers.

Figure S5. Changes in cell proportions during PBMC aging.

A. Percentage of major immune cells in PBMCs in YA (n = 8) and AA (n = 8) from scRNA-seq data.

B. Percentage of major immune cells in CD45⁺ cells in YA (n = 5) and AA (n = 5) from mass cytometry data.

C. Bar chart of the relative percentage of NK subsets from scRNA-seq data.

D. Bar chart of the relative percentage of NK subsets from mass cytometry data.

E. Bar chart of the relative percentage of BC subsets from scRNA-seq data.

F. Bar chart of the relative percentage of BC subsets from mass cytometry data.

G. Bar chart of the relative percentage of monocyte subsets from scRNA-seq data.

H. Bar chart of the relative percentage of monocyte subsets from mass cytometry data.

I. Percentage of cell subsets in PBMCs in YA (n = 8) and AA (n = 8) from scRNA-seq data.

J. Percentage of cell subsets in PBMC in YA (n = 5) and AA (n = 5) from mass cytometry data.

P values are based on two-tailed Mann-Whitney-Wilcoxon tests between groups.

Figure S6. Changes in transcriptional profiles of T cells and NK cells during aging.

A. UpSet plot showing integrated comparative analysis of downregulated DEGs in major immune cell populations between YA and AA groups. Downregulated DEGs: downregulated in AA, upregulated in YA.

B. Representative GO terms and pathways enriched in downregulated DEGs based on functional enrichment analysis in major immune cell populations. *P* value was derived by a hypergeometric test.

C. Representative GO terms and pathways enriched in downregulated DEGs based on functional enrichment analysis in CD4⁺ T cells. *P* value was derived by a hypergeometric test.

D. UpSet plot showing integrated comparative analysis of upregulated DEGs in CD8⁺ T cells between YA and AA groups. Upregulated DEGs: upregulated in AA, downregulated in YA.

E. Representative GO terms and pathways enriched in upregulated DEGs based on functional enrichment analysis in CD8⁺ T cells. *P* value was derived by a hypergeometric test.

F. Representative GO terms and pathways enriched in downregulated DEGs based on functional enrichment analysis in CD8⁺ T cells. *P* value was derived by a hypergeometric test.

G. Volcano plot showing DEGs of T-mito between YA and AA groups. *P* values were calculated using a paired, two-sided Wilcoxon test and FDR was corrected using the Benjamini-Hochberg procedure.

H. Dot plot showing enriched pathways of upregulated and downregulated DEGs in T-mito cluster during aging. *P* value was derived by a hypergeometric test.

I. Representative GO terms and pathways enriched in upregulated DEGs based on functional enrichment analysis in NK cells. *P* value was derived by a hypergeometric test.

J. Representative GO terms and pathways enriched in downregulated DEGs based on functional enrichment analysis in NK cells. *P* value was derived by a hypergeometric test.

Figure S7. Changes in transcriptional profiles of B cells, monocytes and DCs during aging.

- A. UpSet plot showing the integrated comparative analysis of upregulated DEGs in B cell subsets between YA and AA groups. Upregulated DEGs: upregulated in AA, downregulated in YA.
- B. Representative GO terms and pathways enriched in upregulated DEGs based on functional enrichment analysis in B cell subsets. *P* value was derived by a hypergeometric test.
- C. Representative GO terms and pathways enriched in downregulated DEGs based on functional enrichment analysis in B cell subsets. *P* value was derived by a hypergeometric test.
- D. Representative GO terms and pathways enriched in downregulated DEGs based on functional enrichment analysis in monocyte subsets. *P* value was derived by a hypergeometric test.
- E. UpSet plot showing the integrated comparative analysis of upregulated DEGs in DC subsets between YA and AA groups. Upregulated DEGs: upregulated in AA, downregulated in YA.
- F. Representative GO terms and pathways enriched in upregulated DEGs based on functional enrichment analysis in DC subsets. *P* value was derived by a hypergeometric test.
- G. UpSet plot showing the integrated comparative analysis of downregulated DEGs in DC subsets between YA and AA group. Downregulated DEGs: downregulated in AA, upregulated in YA.
- H. Representative GO terms and pathways enriched in downregulated DEGs based on functional enrichment analysis in DC subsets. *P* value was derived by a hypergeometric test.
- I. Violin plots showing the distribution of normalized expression levels of selected aging-associated genes in DC cluster (*CASP4* and *IFITM3* in all DC, *AHR* in cDC2, *MALAT1* in pDC) between YA and AA groups.
- J. Heatmap showing biased DEGs within the cDC2-A and cDC2-B cluster.
- K. Violin plots showing the distribution of normalized expression levels of selected aging-associated genes in cDC2-A and cDC2-B cluster.

Figure S8. Changes in chromosomal accessibility during aging.

- A. t-SNE projection of canonical markers, including *CD3E*, *CD4*, *CD8A*, *NCAM1*, *NKG7*, *CD19*, *CD20*, *CD14*, *FCGR3A*, *ITGA2B*.
- B. t-SNE projections of NK cells and T cells derived from scATAC-seq data.
- C. t-SNE projections of B cells derived from scATAC-seq data.
- D. t-SNE projections of monocytes and DCs derived from scATAC-seq data.
- E. Venn diagram showing the integrated comparative analysis of downregulated differentially expressed transcription factors (DETs) in CD4⁺ T cell subsets between YA and AA group. Downregulated DETs: downregulated in AA, upregulated in YA.
- F. Venn diagram showing the integrated comparative analysis of downregulated DETs in CD8⁺ T cell subsets between YA and AA group. Downregulated DETs: downregulated in AA, upregulated in YA.
- G. Venn diagram showing the integrated comparative analysis of downregulated DETs in NK subsets between YA and AA group. Downregulated DETs: downregulated in AA, upregulated in YA.
- H. Mean scATAC-seq coverage at *NRF1* loci in all cells.
- I. Mean scATAC-seq coverage at *ELK4* loci in Memory B cells.
- J. Mean scATAC-seq coverage at *GZMB* loci in CD8 CTL.
- K. Mean scATAC-seq coverage at *IL1B* loci in CD14 MC.

- L. Mean scATAC-seq coverage at *TNF* loci in CD16 MC.
- M. Mean scATAC-seq coverage at *CXCL8* loci in CD16 MC.

Figure S9. Abnormal TCR and BCR repertoire during aging.

- A. Bar plot showing specific TRA usage in the YA and AA groups.
- B. Bar plot showing specific TRB usage in the YA and AA groups.
- C. Bar plot showing specific IGH usage in the YA and AA groups.
- D. Bar plot showing specific IGK usage in the YA and AA groups.
- E. Bar plot showing specific IGL usage in the YA and AA groups.
- F. Bar plot showing the relative percentage of each isotype in the YA and AA groups.
- G. Bar plot showing the ratio of (*IGHA* + *IGHG*) to (*IGHD* + *IGHM*) among the YA and AA groups (n = 8/group). P values are based on two-tailed Mann-Whitney-Wilcoxon tests between groups.
- H. Chord diagram showing the pairing of V and J segments within TRB subset from the YA group. Chord widths represent the proportion of sequences with a given V (colored) and J (gray) segment pairing.
- I. Chord diagram showing the pairing of V and J segments within IGH subset from the YA group. Chord widths represent the proportion of sequences with a given V (colored) and J (gray) segment pairing.

Figure S10. Clusters of major immune cell populations derived from mass cytometry data in cohort-2.

- A. t-SNE projections of PBMCs.
- B. t-SNE plots segregated by YH, AH, YCO and ACO groups.
- C. t-SNE projection of canonical markers, including CD3, CD4, CD8A, CD11C, CD56, CD57, CD19, CD20, CD14, CD16, HLA-DRA, CD123.

Figure S11. Re-Clustering of cell subsets derived from mass cytometry data in cohort-2.

- A. t-SNE projections of T cell subsets.
- B. t-SNE projections of NK cell subsets.
- C. t-SNE projections of B cell subsets.
- D. t-SNE projections of monocyte subsets.
- E. t-SNE projections of DC subsets derived.
- F. t-SNE projection of canonical markers in T cell subsets.
- G. t-SNE projection of canonical markers in NK cell subsets.
- H. t-SNE projection of canonical markers in B cell subsets.
- I. t-SNE projection of canonical markers in monocytes subsets.
- J. t-SNE projection of canonical markers in DC subsets.
- K. Heatmap showing mean population expression levels of all markers.

Figure S12. Poor outcome upon COVID-19 infection is associated with imbalanced cellular aging.

- A. Bar chart of the relative percentage of all cell subsets derived from mass cytometry data in cohort-2. HC includes YH (n = 2) and AH (n = 2); CO includes YCO n = 2 and ACO n = 2.
- B. Bar chart of the relative percentage of T cell subsets derived from mass cytometry data in cohort-2.
- C. Percentage of CD8 Naive T cells in CD45⁺ cells derived from mass cytometry data between HC (n = 4) and CO (n = 4) groups.

- D. Percentage of CD8 CTL in CD45⁺ cells derived from mass cytometry data between HC (n = 4) and CO (n = 4) groups.
- E. Bar chart of the relative percentage of B cells subsets derived from mass cytometry data between HC and CO group.
- F. Percentage of memory BC in CD45⁺ cells between HC (n = 4) and CO (n = 4) groups.
- G. Percentage of ASC in CD45⁺ cells between HC (n = 4) and CO (n = 4) groups.
- H. Bar chart of the relative percentage of NK subsets derived from mass cytometry data between HC and CO group.
- I. Bar chart of the relative percentage of monocyte subsets derived from mass cytometry data between HC and CO group.
- J. Percentage of intermediate monocytes in CD45⁺ cells between HC (n = 4) and CO (n = 4) groups.
- K. Bar chart of the relative percentage of DC subsets derived from mass cytometry data between HC and CO group.
- L. Percentage of pDC in CD45⁺ cells between HC (n = 4) and CO (n = 4) groups.
- M. Bar chart of the relative percentage of all cell subsets derived from mass cytometry data between YH, AH and ACO groups.
- N. Bar chart of the relative percentage of all cell subsets derived from mass cytometry data between YCO and ACO groups.
- O. Bar chart of the relative percentage of T cell subsets derived from mass cytometry data between YCO and ACO groups.
- P. Bar chart of the relative percentage of NK subsets derived from mass cytometry data between YCO and ACO groups.
- Q. Bar chart of the relative percentage of BC subsets derived from mass cytometry data between YCO and ACO groups.
- R. Bar chart of the relative percentage of monocyte subsets derived from mass cytometry data between YCO and ACO groups.
- S. Bar chart of the relative percentage of DC subsets derived from mass cytometry data between YCO and ACO groups.
- P values are based on two-tailed Mann-Whitney-Wilcoxon tests between groups.

Figure S13. Clusters of major immune cell populations derived from scRNA-seq data in cohort-3.

- A. t-SNE projections of PBMCs.
- B. t-SNE plots segregated by YH, AH, YCR and ACR groups.
- C. t-SNE projection of canonical markers, including *CD3E*, *CD4*, *CD8A*, *STMN1*, *CCR7*, *FOXP3*, *AQP3*, *CCR6*, *GZMK*, *GZMB*, *NCAM1*, *B3GAT1*, *FCGR3A*, *HBB*, *PF4*, *CD19*, *MS4A1*, *IL4R*, *CD27*, *MZB1*, *ITGAX*, *CD14*, *CLEC9A*, *CD1c*, *CLEC4C*.

Figure S14. Aging and SARS-CoV-2 infection are characterized by similar hyper-inflammatory states.

- A. Heatmaps showing scaled expression of discriminative gene sets for each cell type and cell subset in cohort-3. Color scheme is based on z-score distribution from -3 (purple) to 3 (yellow).
- B. Violin plot showing the distribution of normalized expression levels of *NFATC1* in CD4 Naive cells cluster between YH and AH groups.
- C. Violin plot showing the distribution of normalized expression levels of *ITGB1* in CD4 Naive cells cluster between YA and AH groups.
- D. Violin plot showing the distribution of normalized expression levels of *PP1B* in CD4 Naive cells cluster between YH and AH groups.

- E. Violin plot showing the distribution of normalized expression levels of *DPP4* in CD4 Naive cells cluster between YH and AH groups.
- F. Bar charts of the relative percentage of all cell subsets between YH, AH and ACR groups (left), YCR and ACR groups (right).

Figure S15. Cell-cell interactions associated with disease recovering events.

A-B. Dot plots showing specific differentially expressed ligand–receptor interactions between YA and AA groups based on Log₂ FC across ligands. Ligand–receptor interactions are shown for TC-MC interactions (A), BC-MC interactions (B). GO terms associated with the functions of the ligands and receptors are labeled to the left.

Supplementary Table Legends

Table S1. Sample information of single-cell PBMCs collected from three separate cohorts for scRNA-seq, CyTOF, scATAC-seq and scTCR/BCR-seq.

Table S2. Antibodies used in CyTOF analysis.

Table S3. Cell clustering strategy in scRNA-seq, CyTOF, scATAC-seq.

Table S4. DEGs in five major immune cells between AA and YA groups.

Table S5. DEGs in CD4⁺ TC, CD8⁺ TC and T-mito subset between AA and YA groups.

Table S6. DEGs in CD4⁺ TC subpopulation between AA and YA groups.

Table S7. DEGs in CD8⁺ TC subpopulation between AA and YA groups.

Table S8. DEGs in NK subpopulation between AA and YA groups.

Table S9. DEGs in BC subpopulation between AA and YA groups.

Table S10. DEGs in MC subpopulation between AA and YA groups.

Table S11. DEGs in DC subpopulation between AA and YA groups.

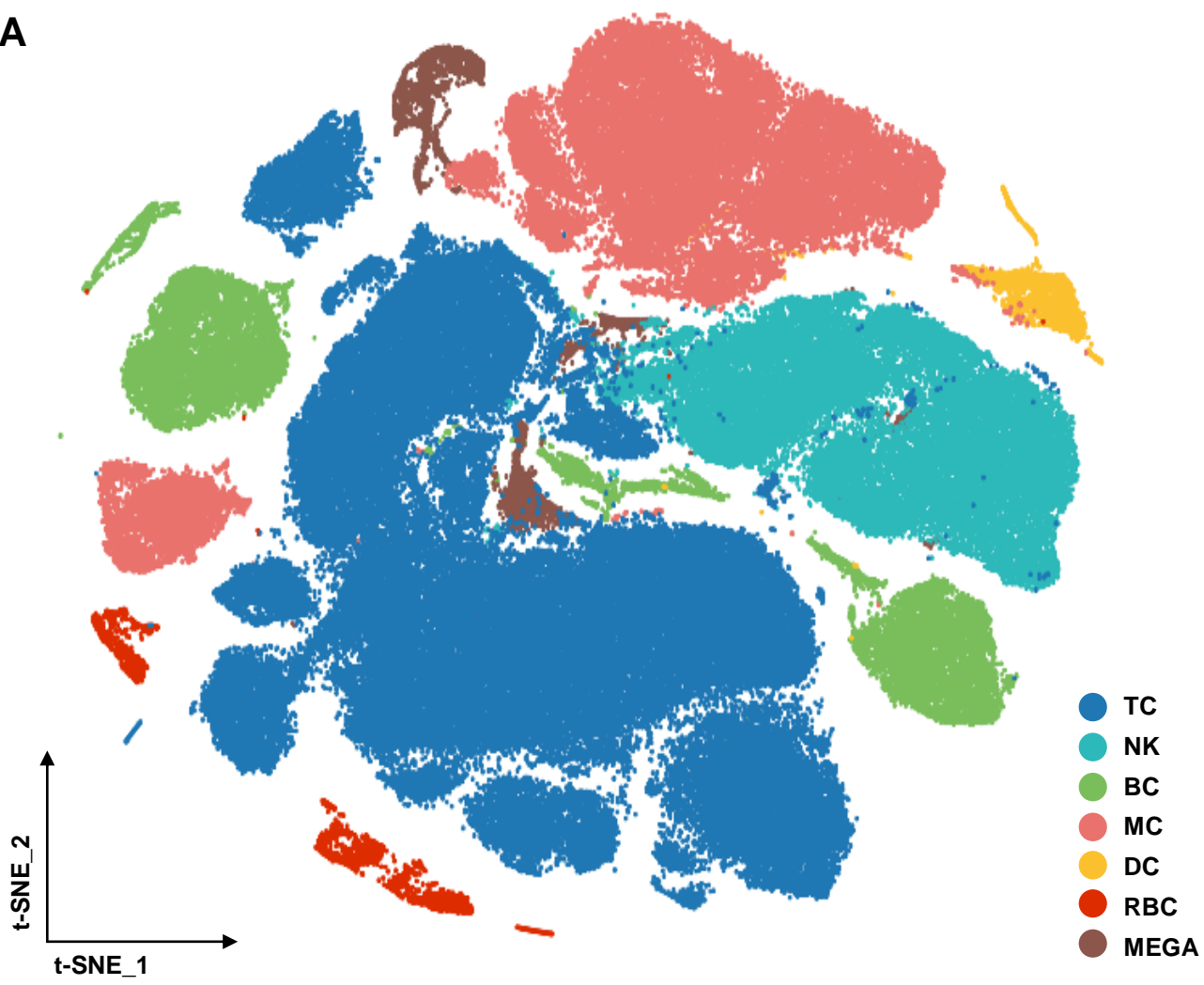
Table S12. DEGs in clonal TC and BC between AA and YA groups.

Table S13. DEGs in TC between AH and YH groups (A), YCR and YH groups (B), ACR and AH groups (C), ACR and YCR groups (D).

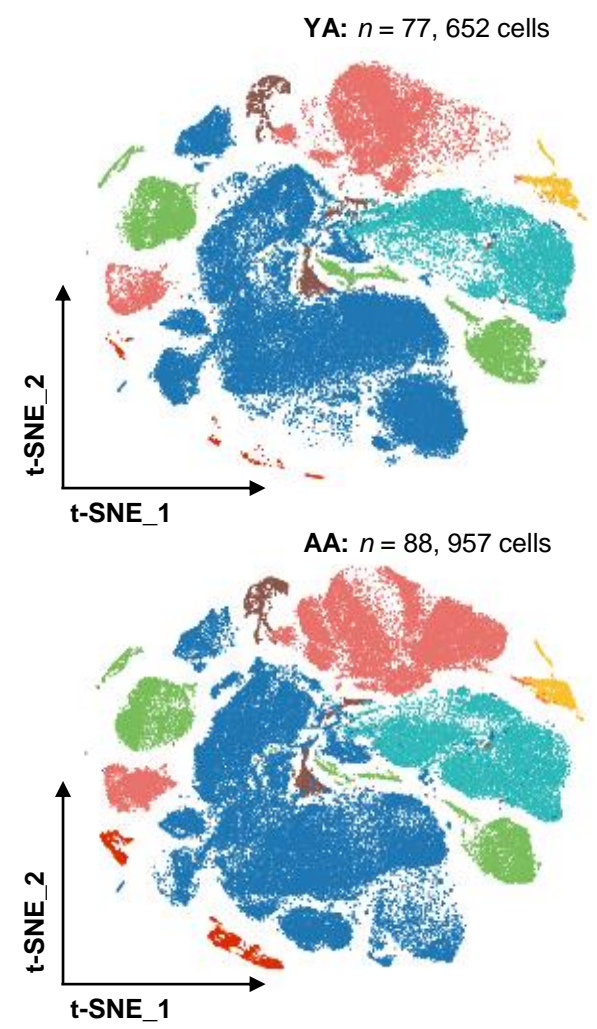
Table S14. DEGs in MC between AH and YH groups (A), YCR and YH groups (B), ACR and AH groups (C), ACR and YCR groups (D).

Figure. S1

A



B



C

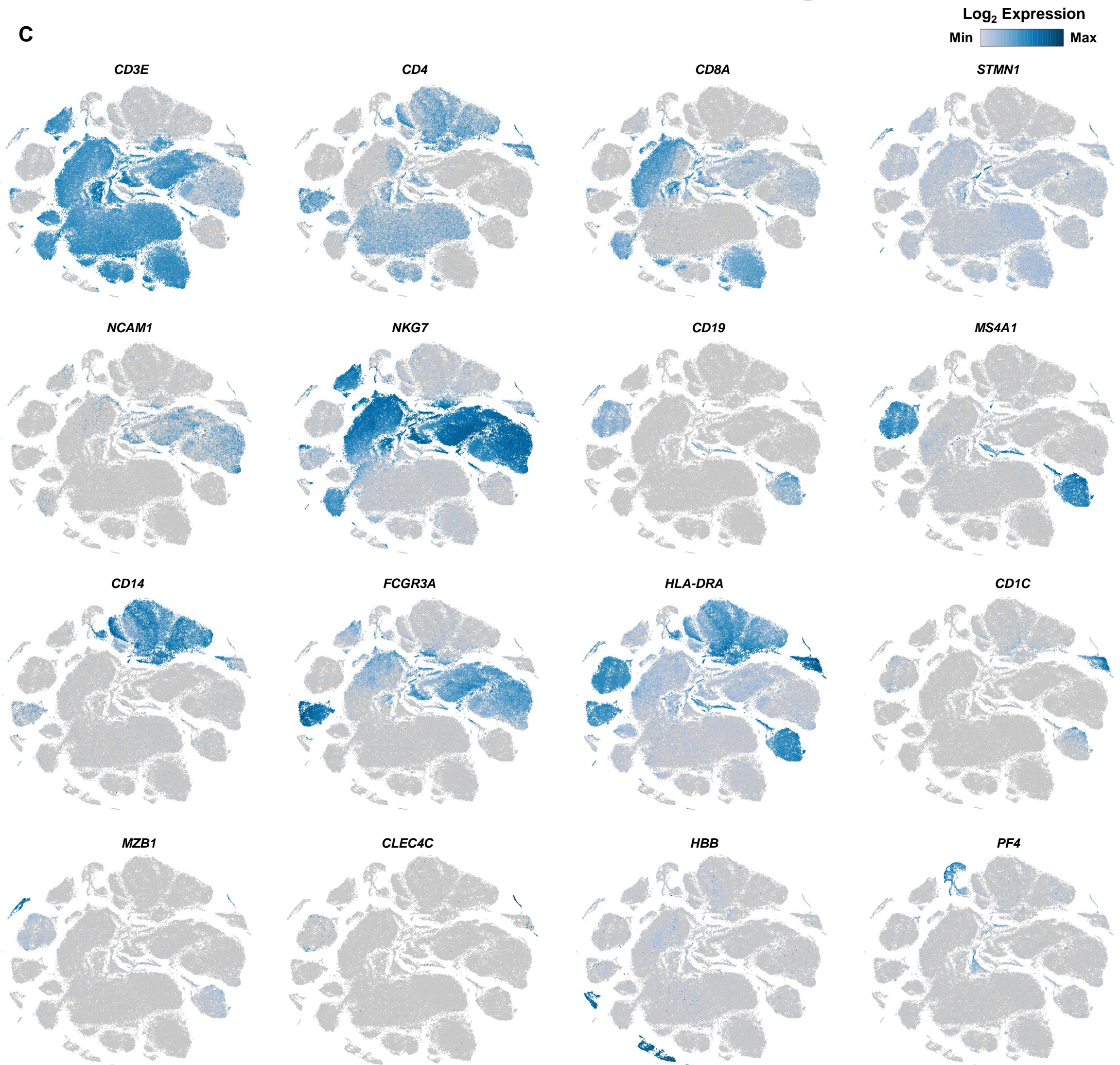


Figure. S3

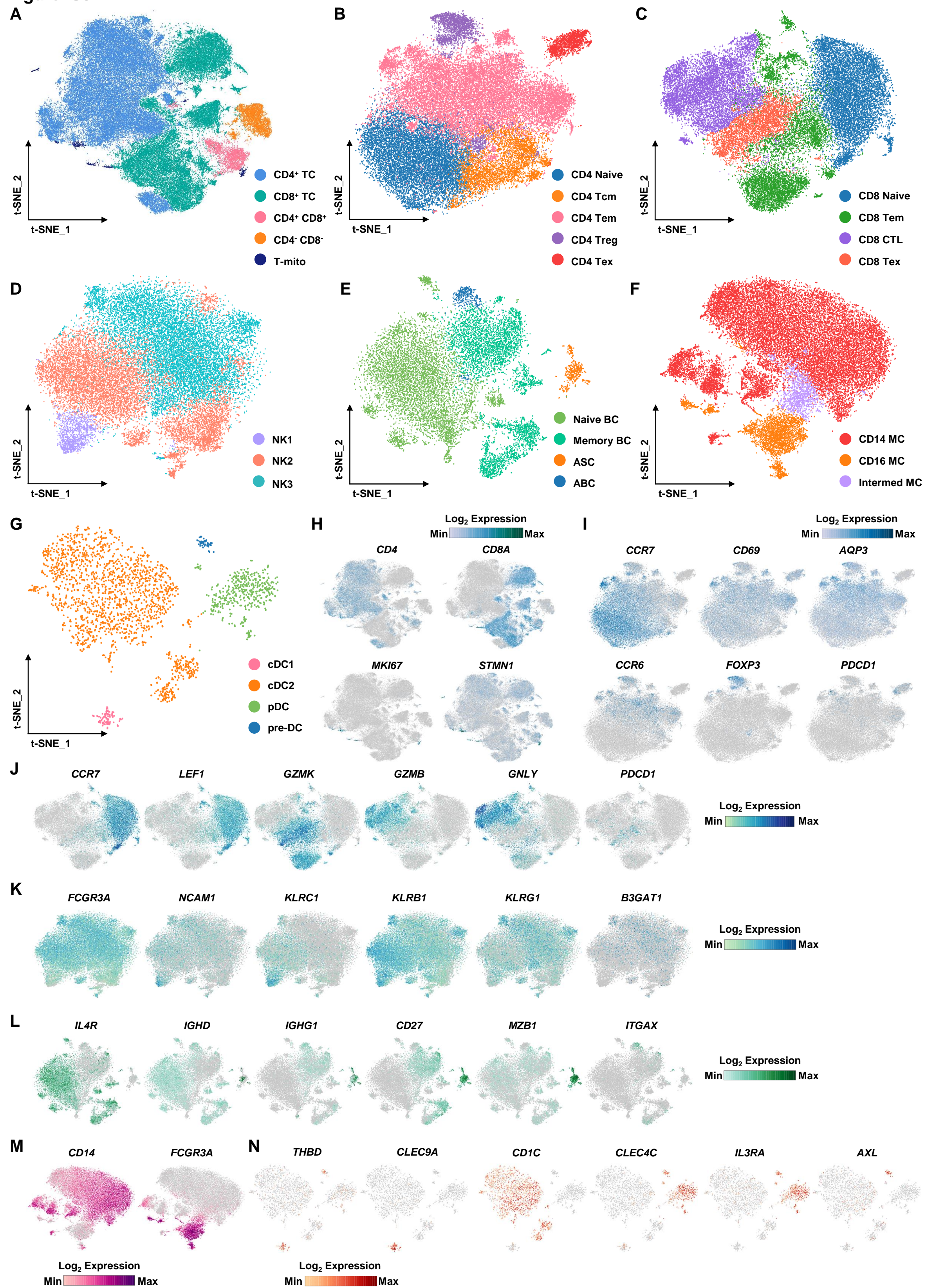


Figure. S5

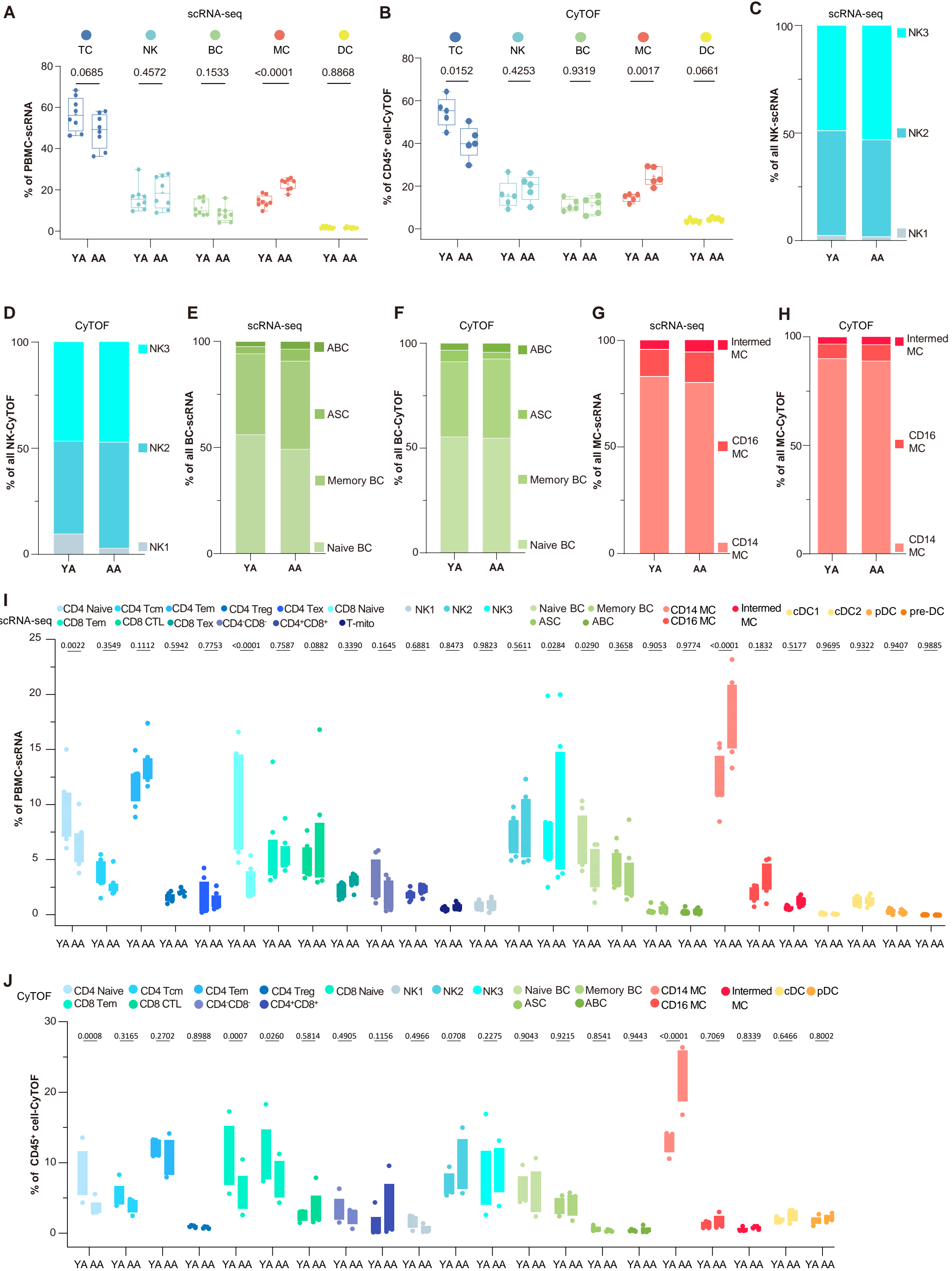


Figure. S6

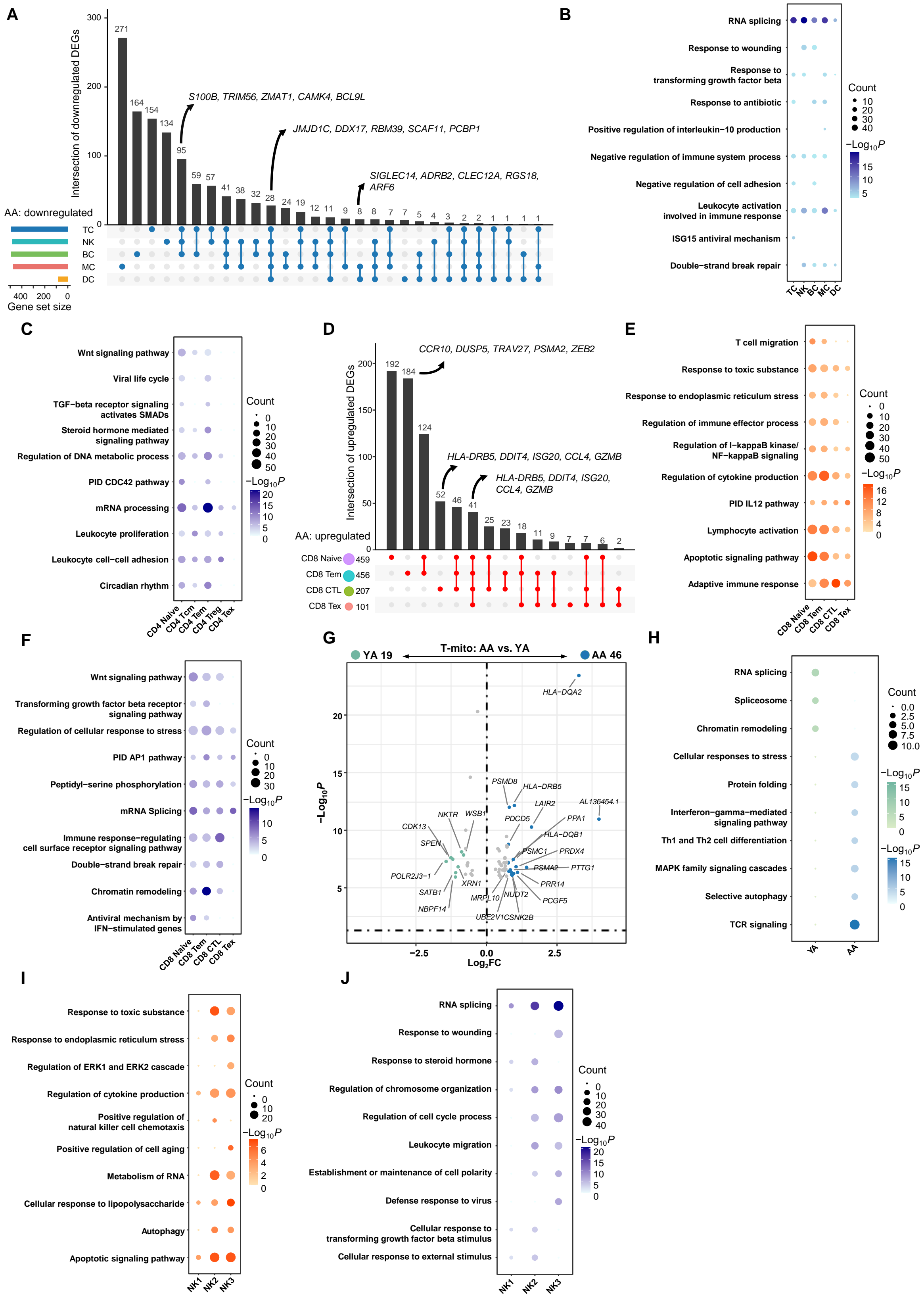
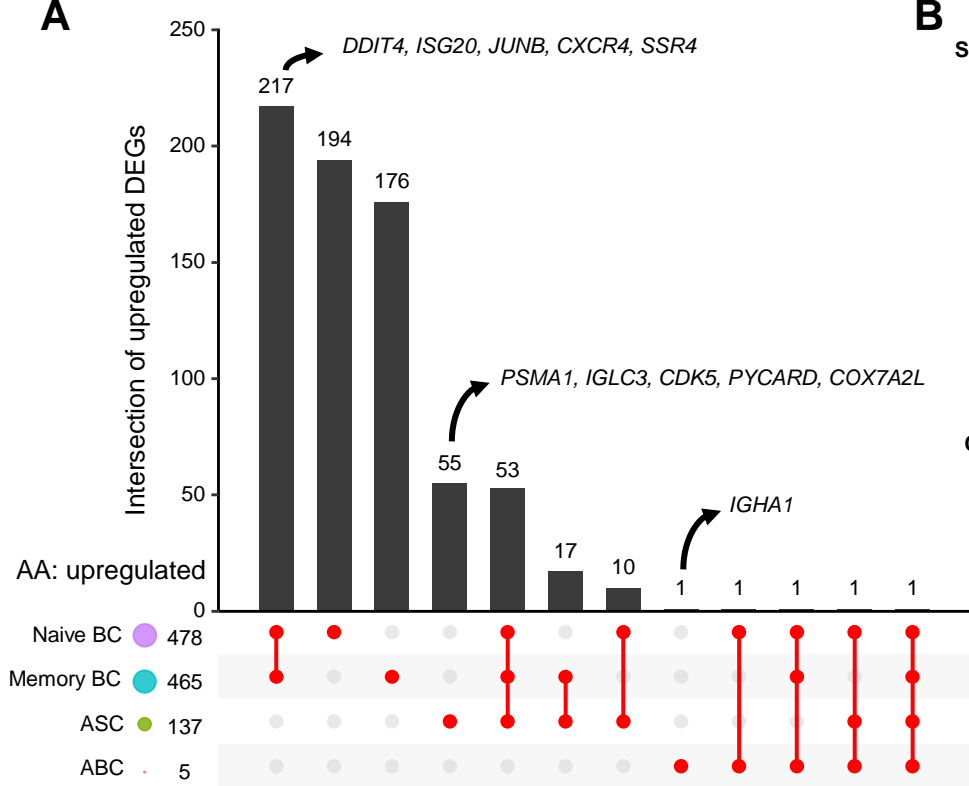
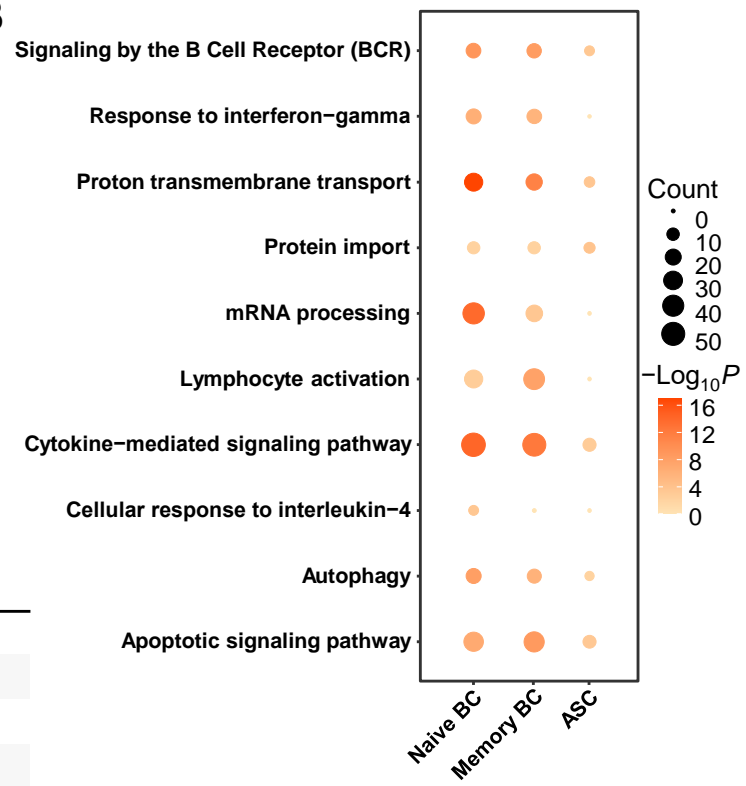


Figure. S7

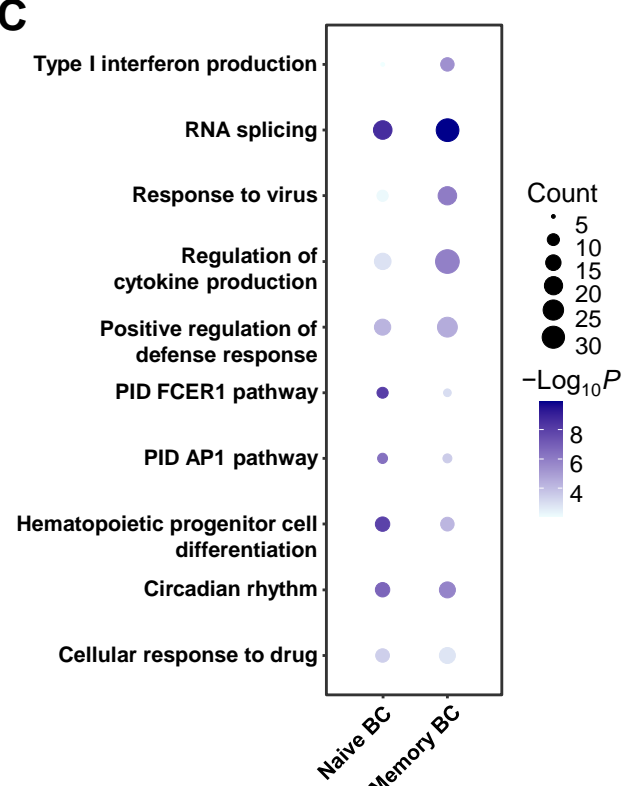
A



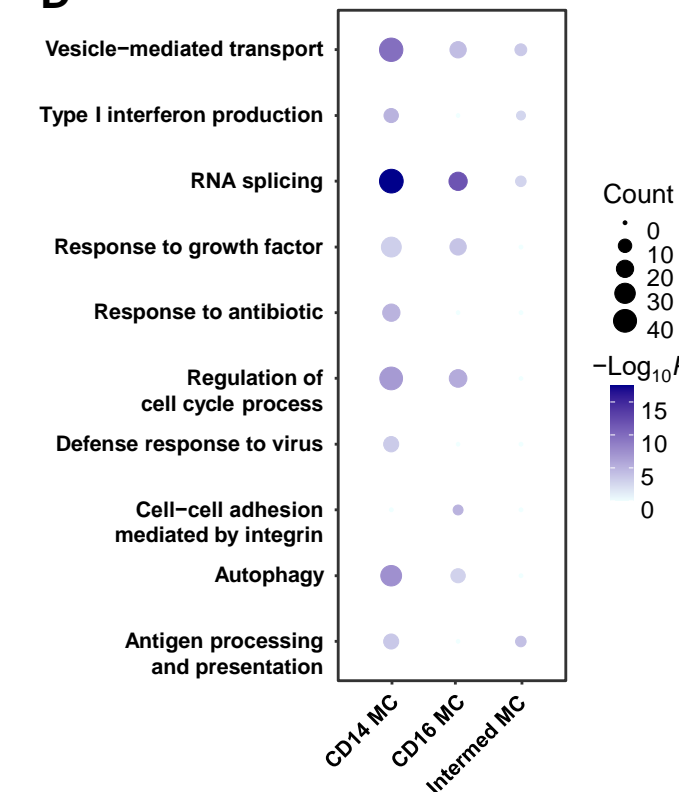
B



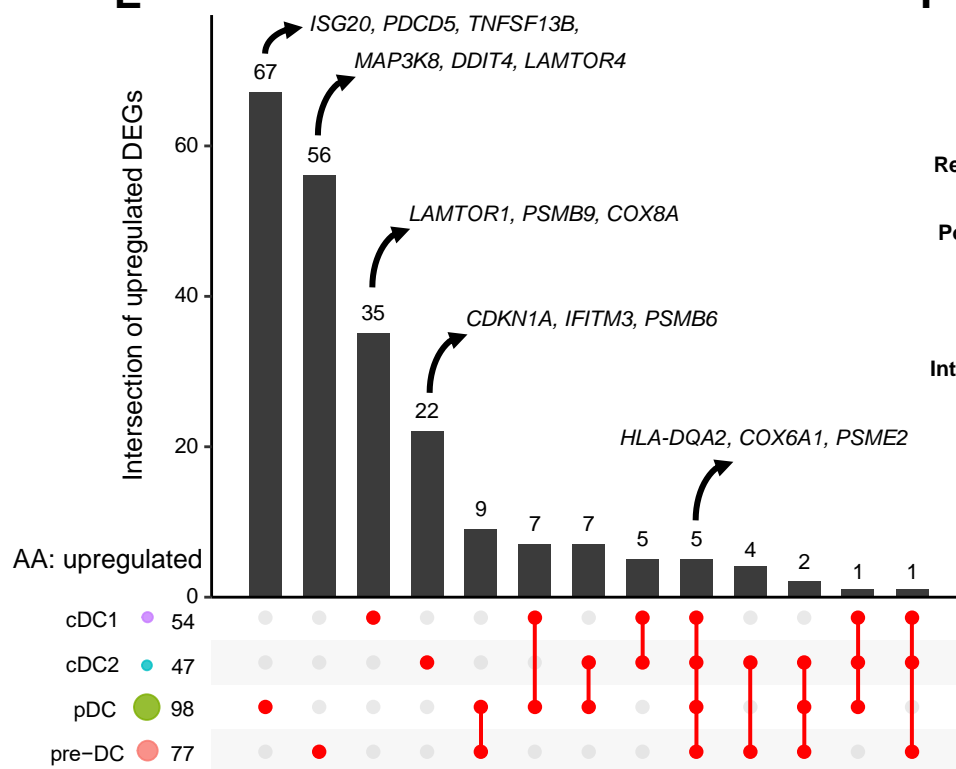
C



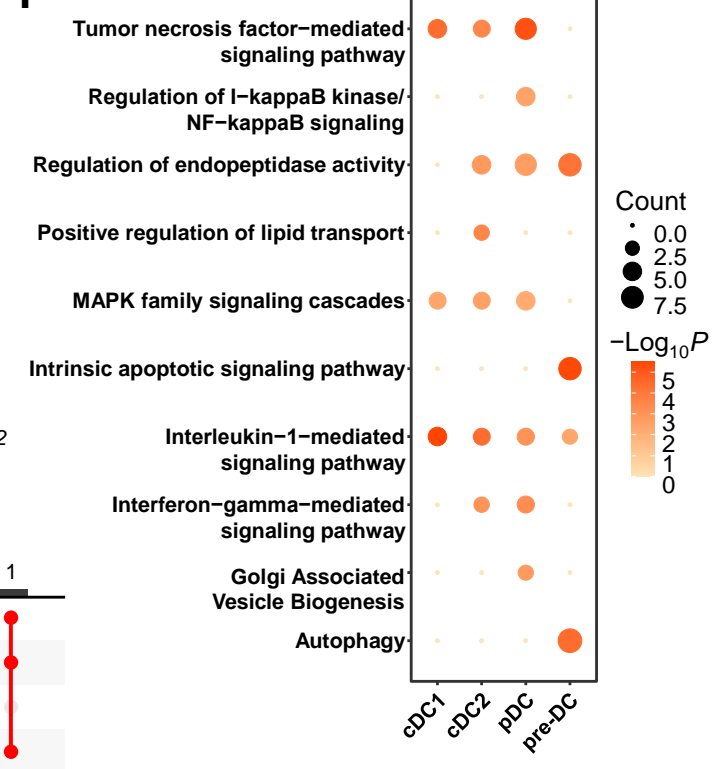
D



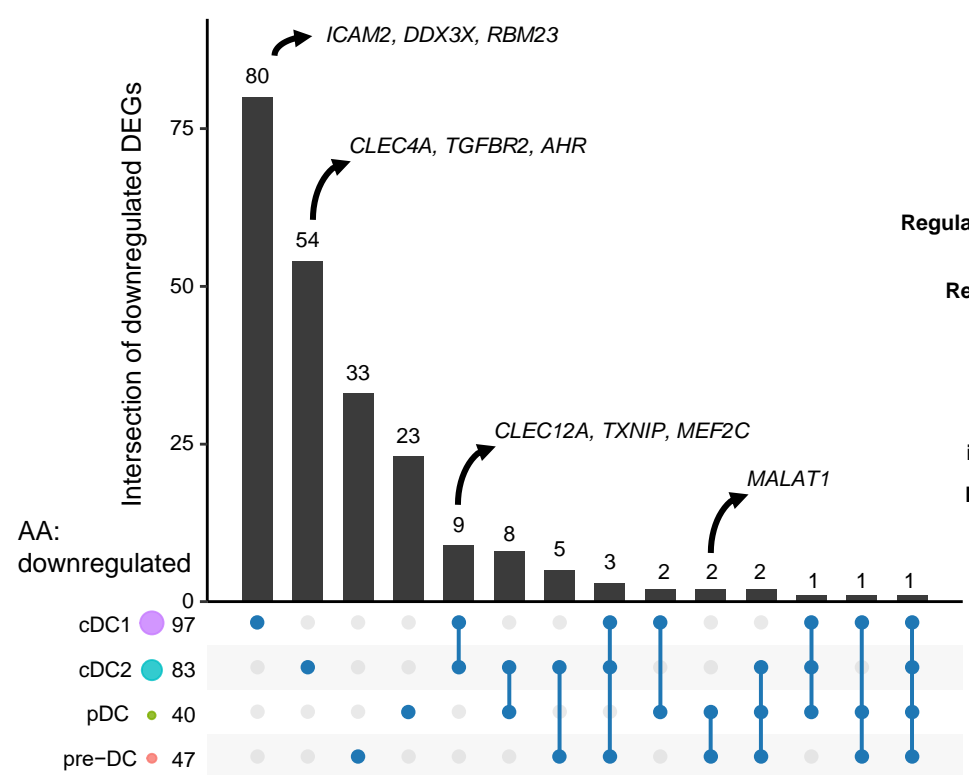
E



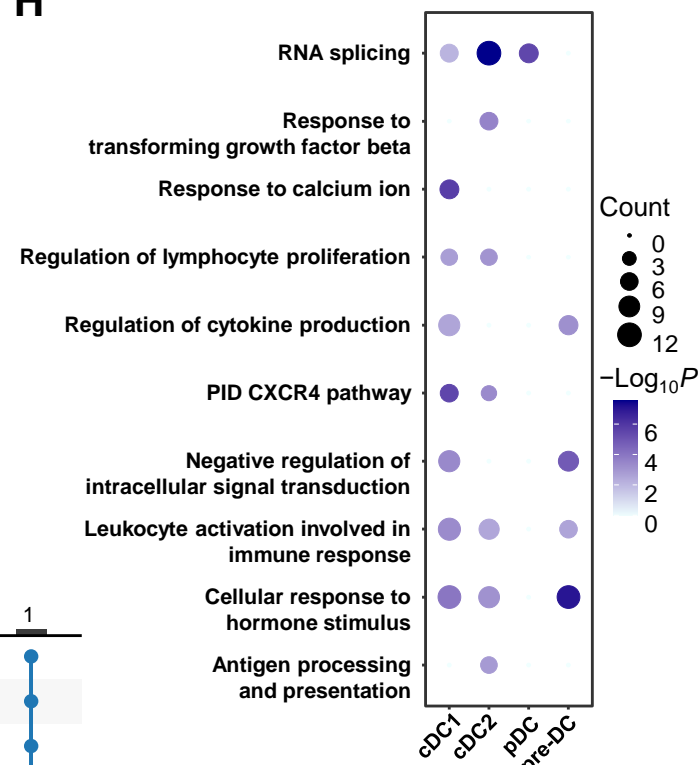
F



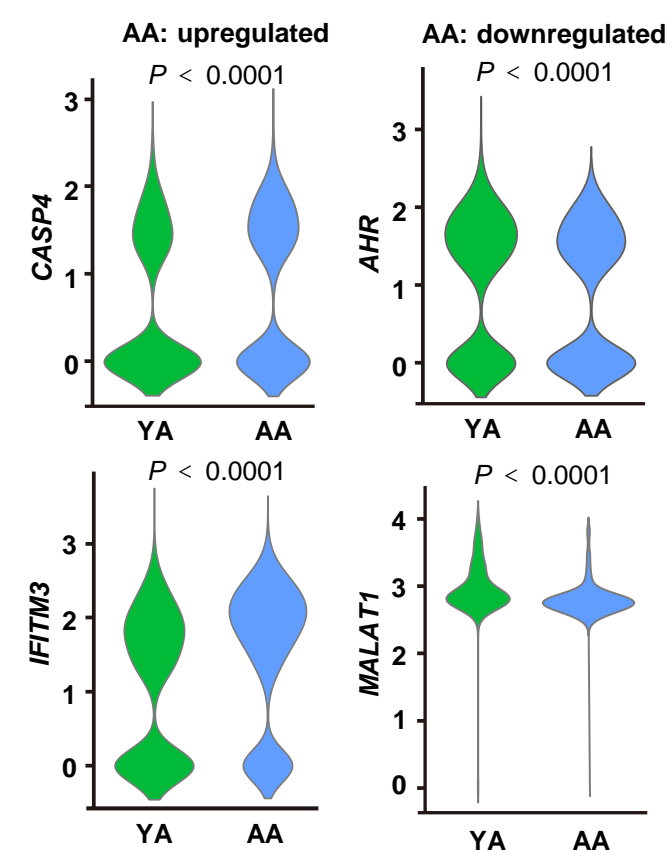
G



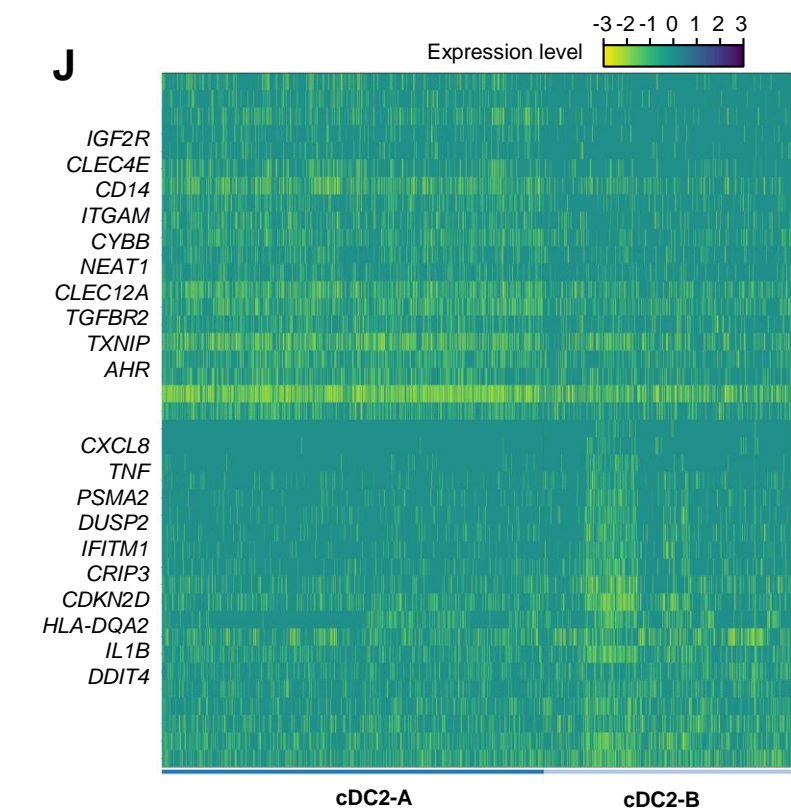
H



I



J



K

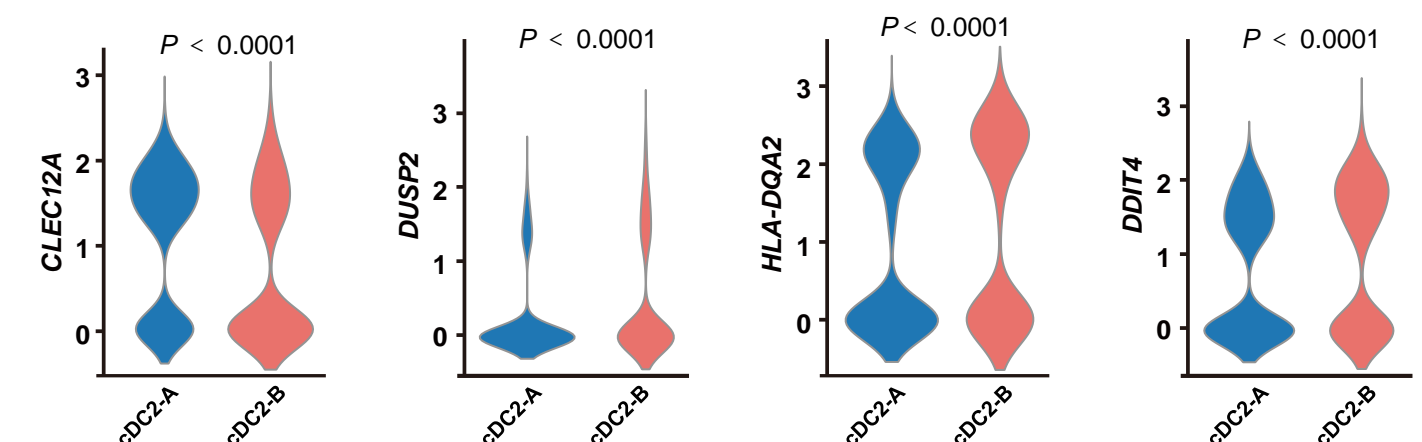


Figure. S8

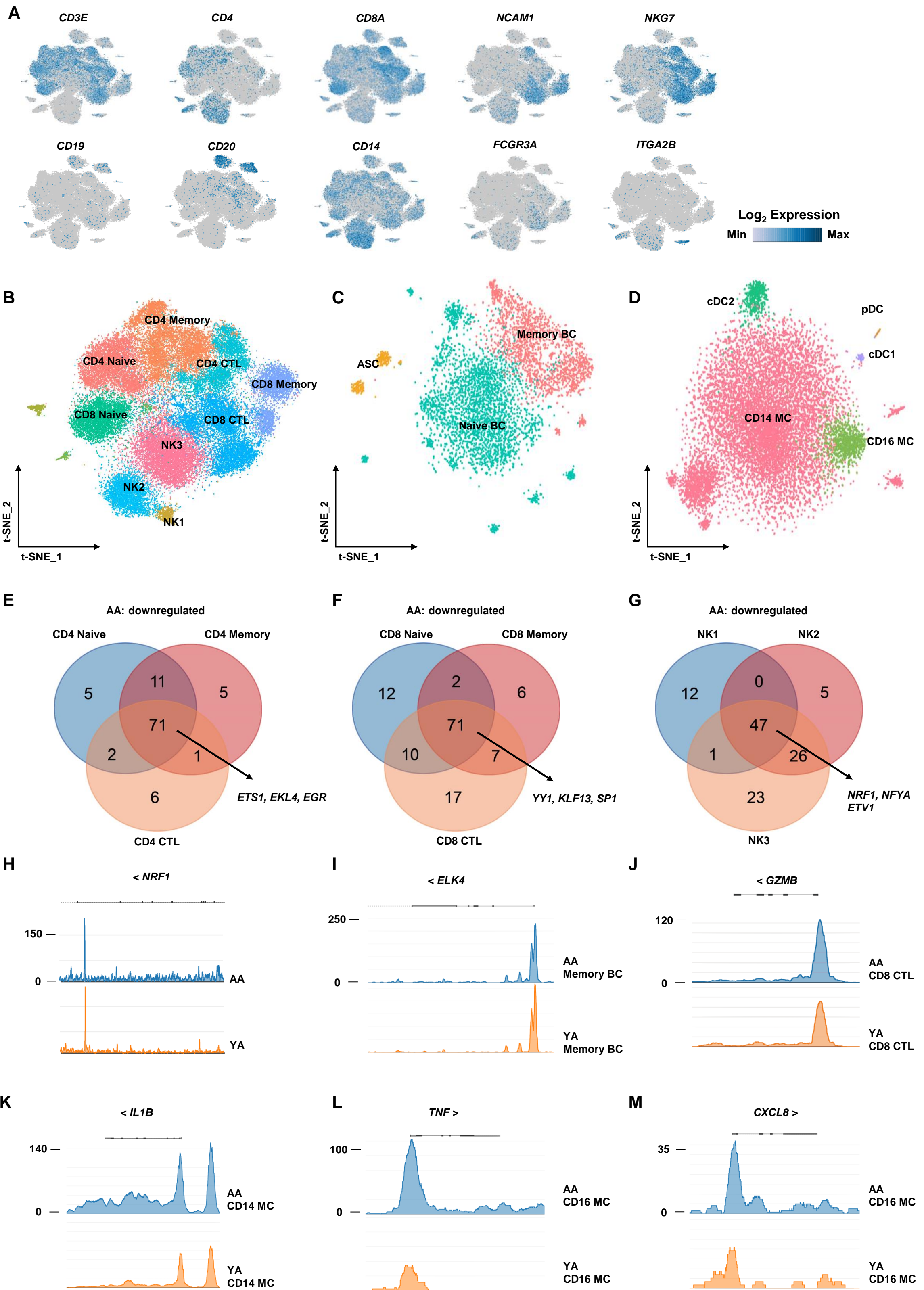


Figure. S9

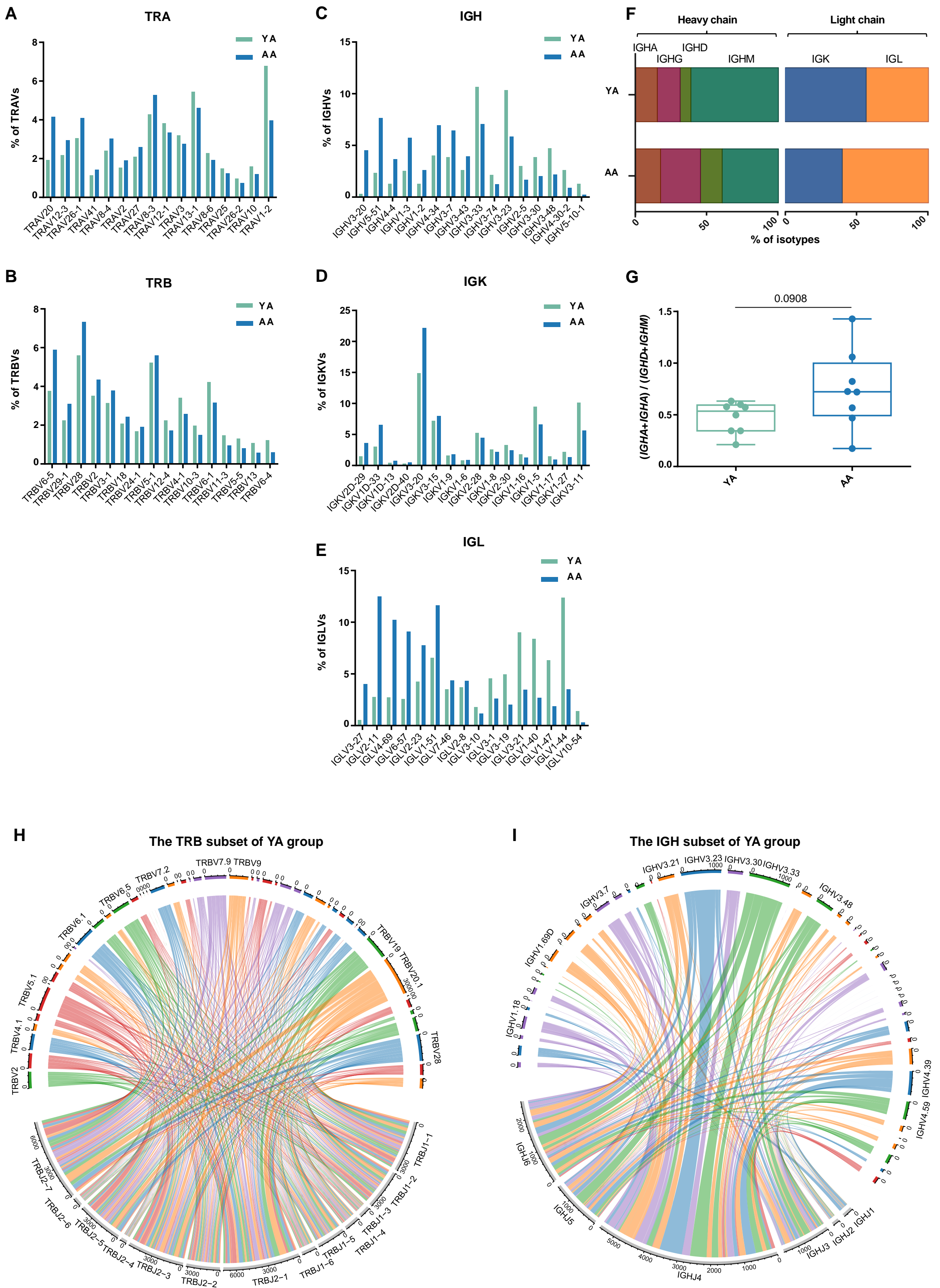
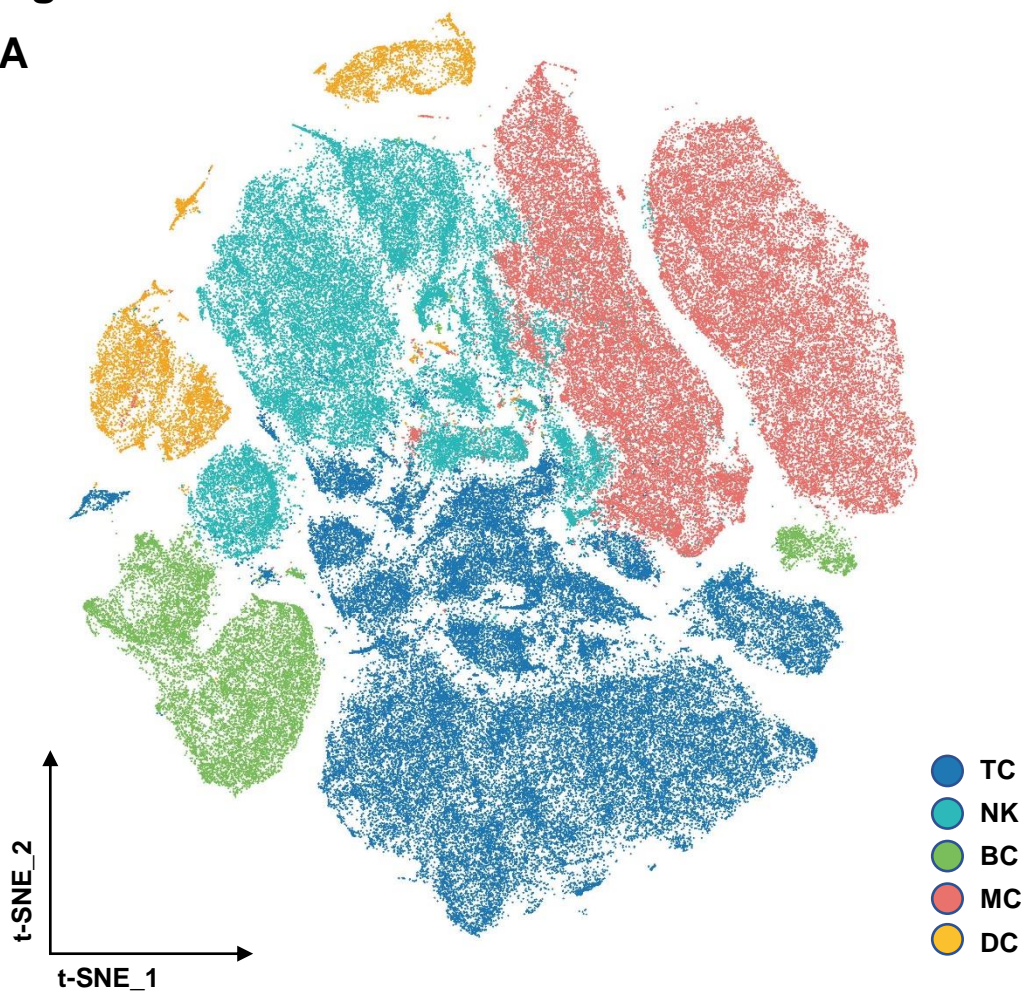
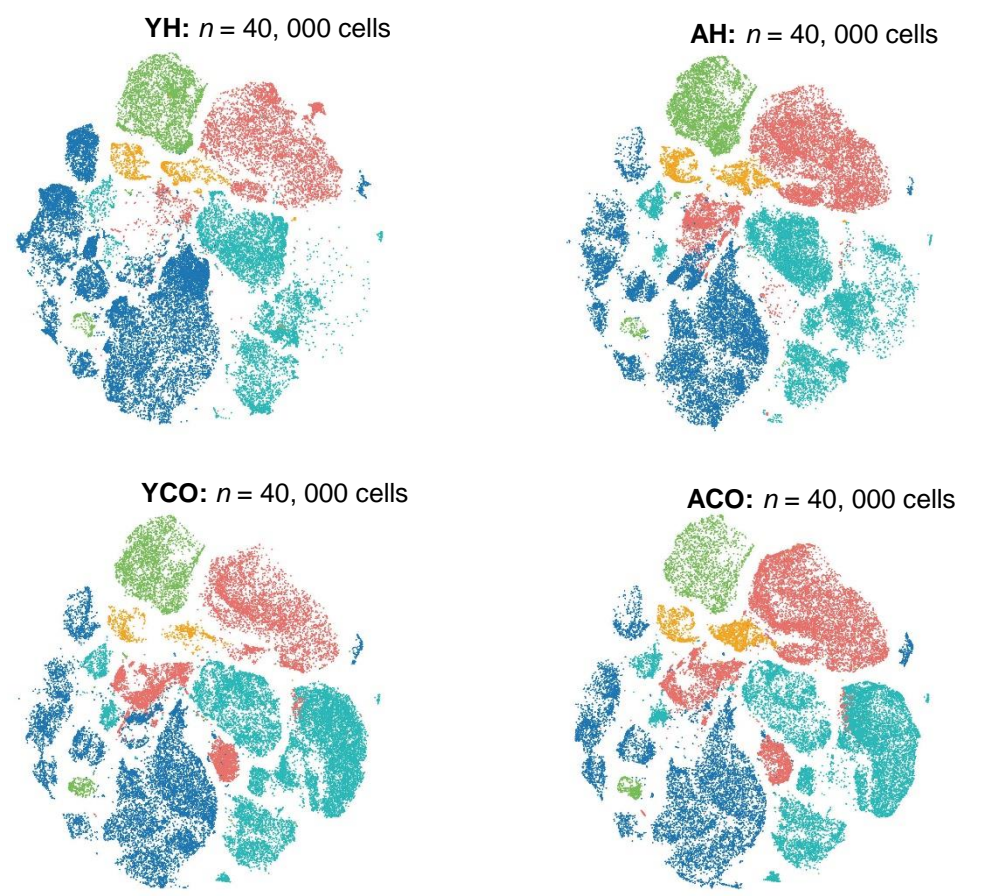


Figure. S10

A



B



C

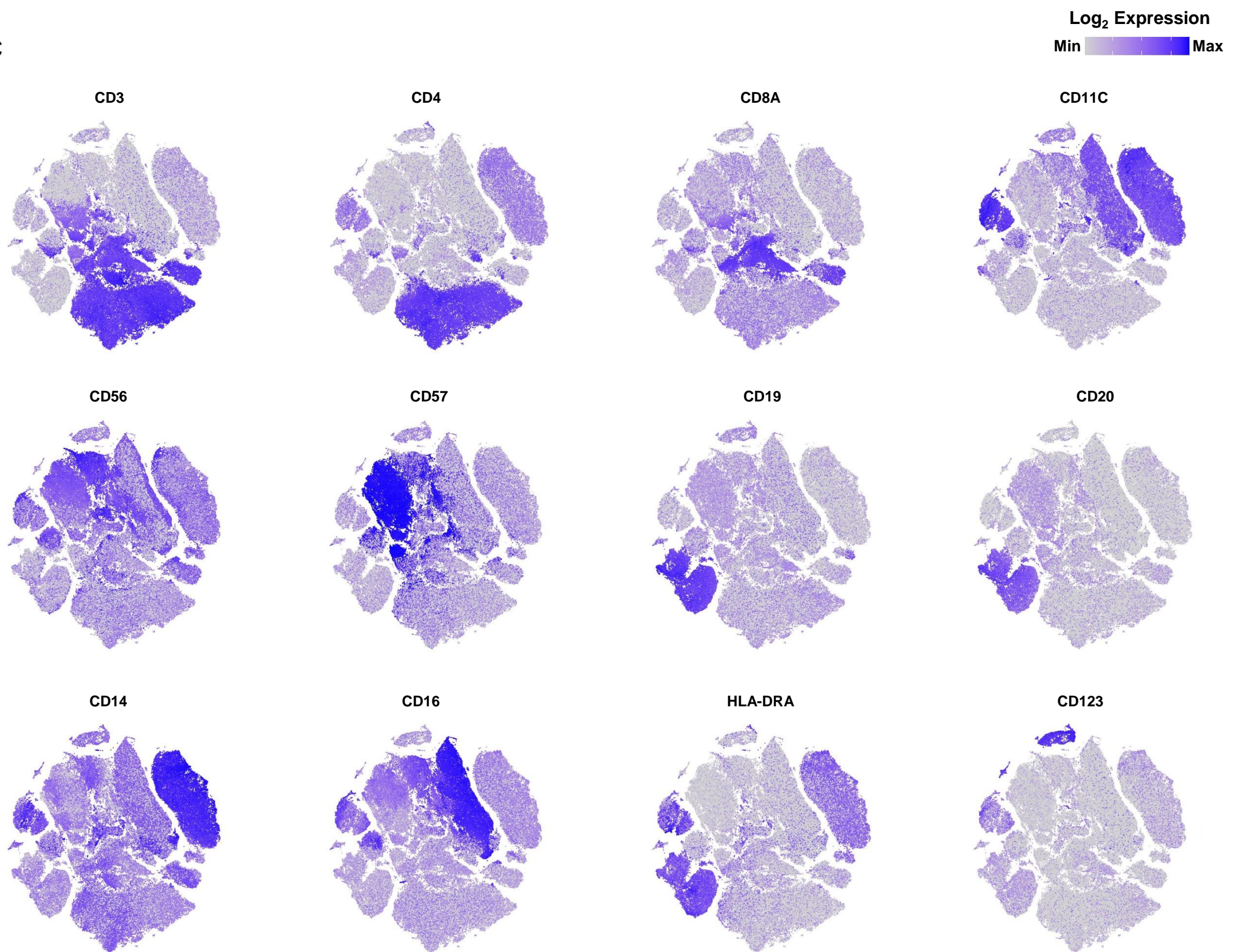


Figure. S12

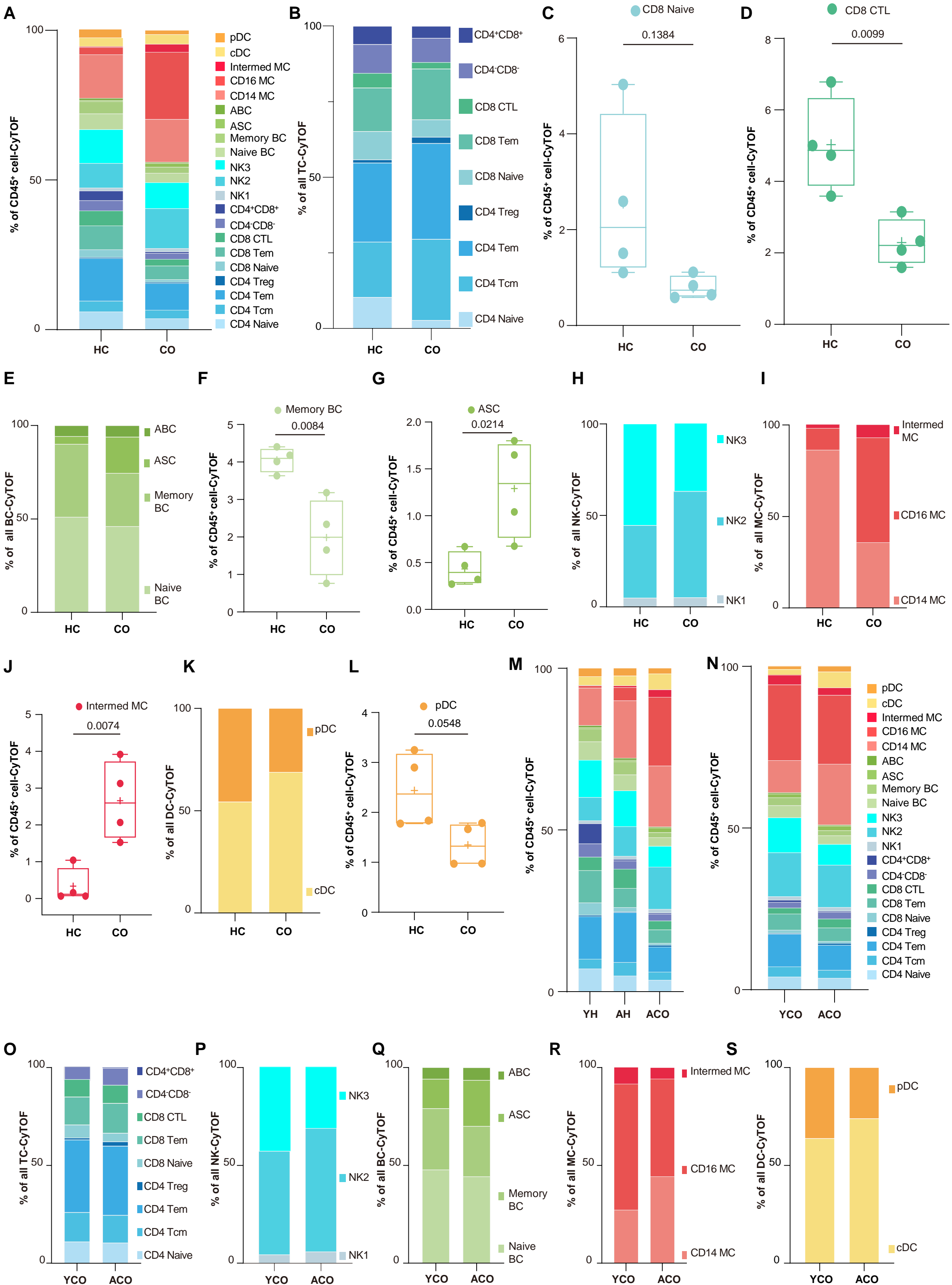
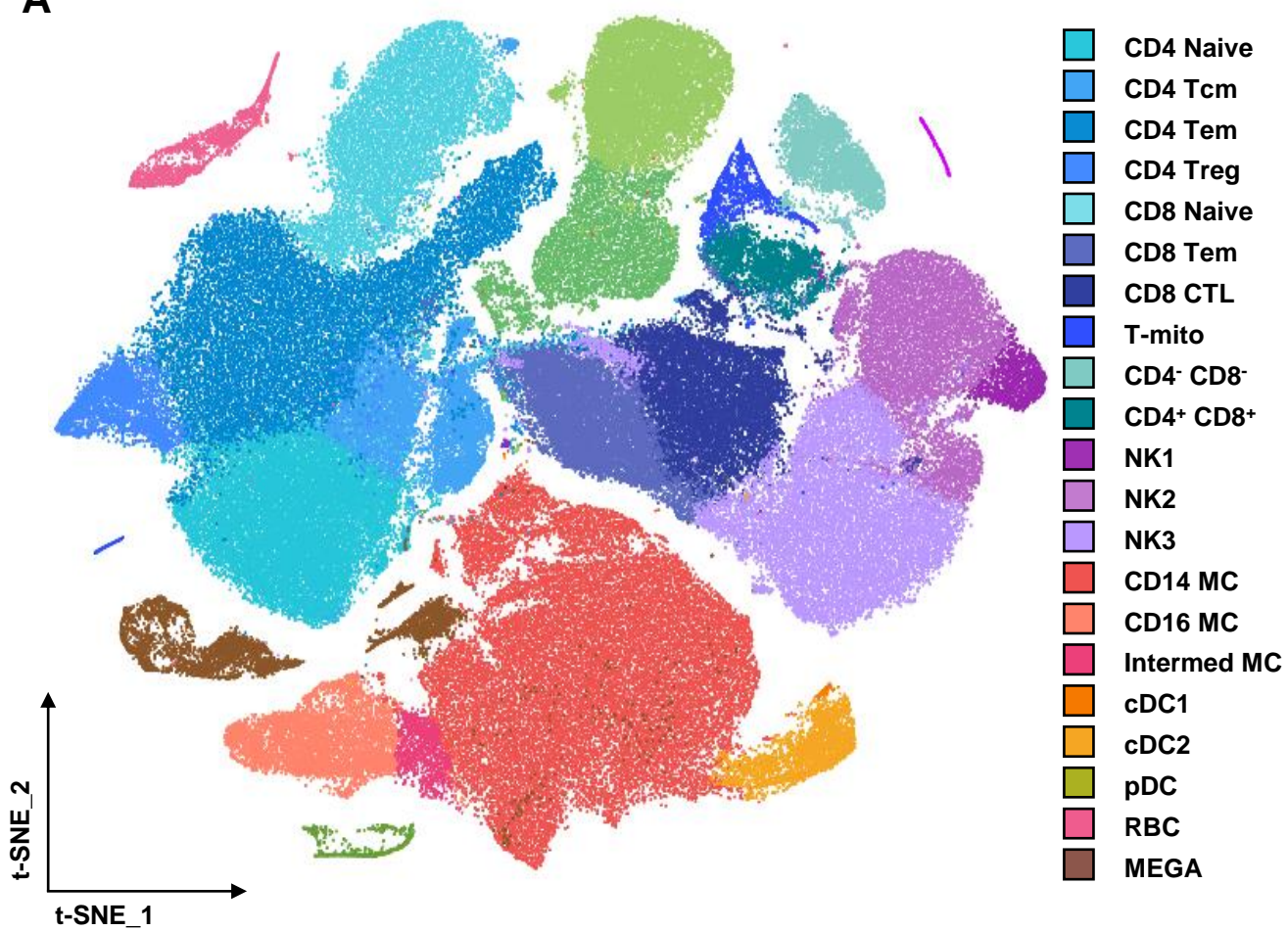
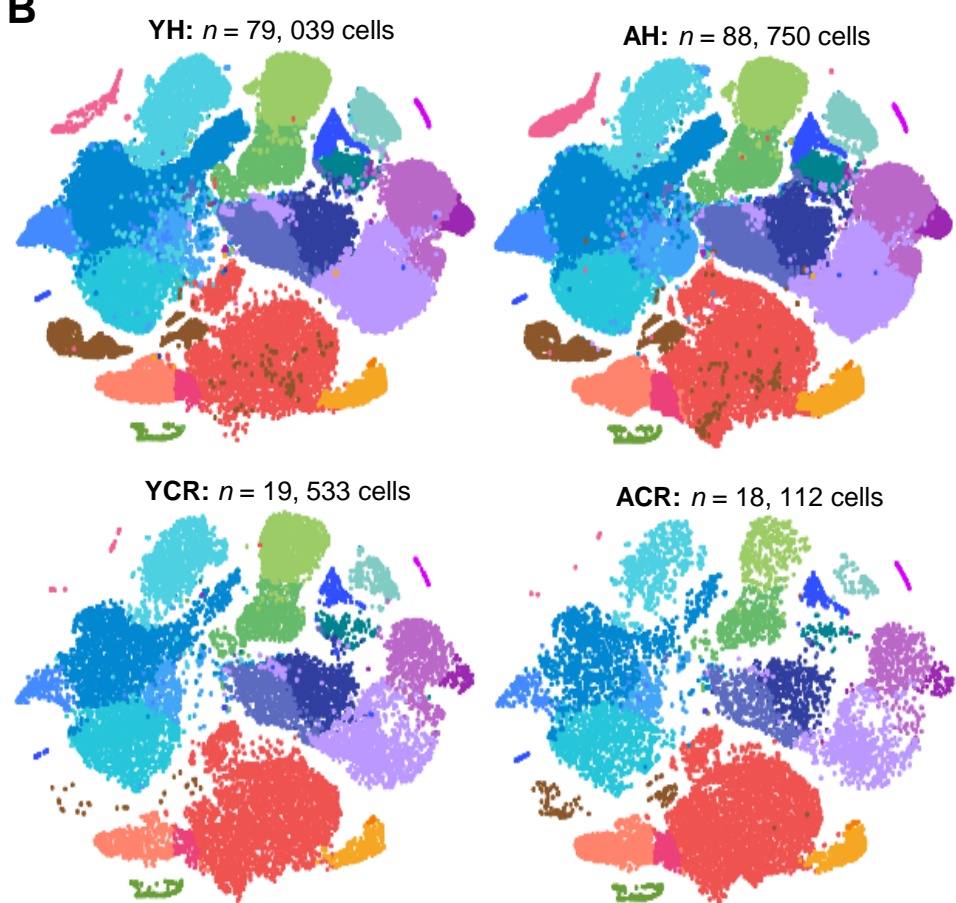


Figure. S13

A



B



C

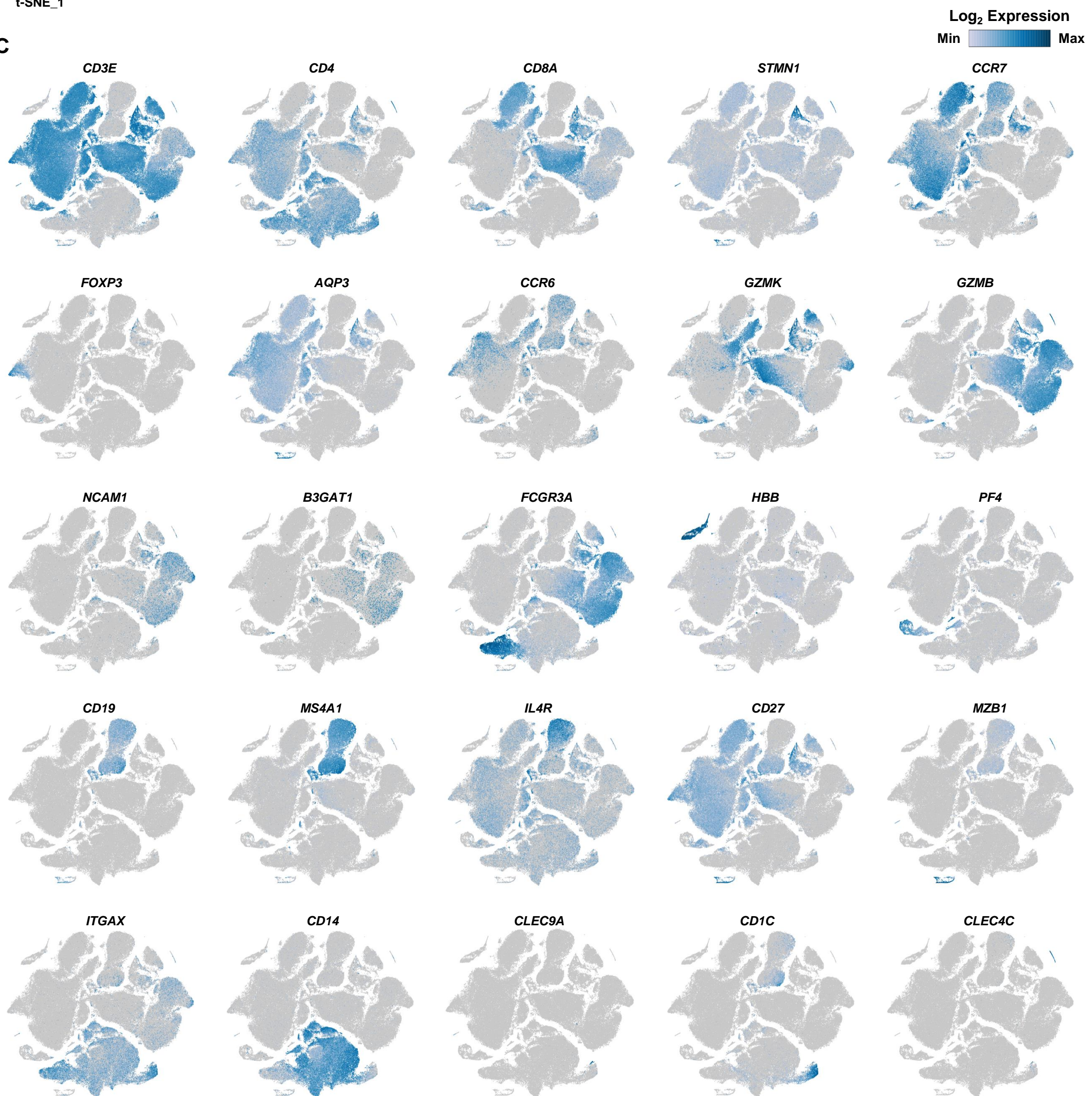


Figure. S15

